1920–1934 *Nucleic Acids Research, 2019, Vol. 47, No. 4* *Published online 22 January 2019*
doi: 10.1093/nar/gkz021

Structure–function relationship in the 'termination upstream ribosomal binding site' of the calicivirus rabbit hemorrhagic disease virus

René Wennesz, Christine Luttermann, Felix Kreher and Gregor Meyers*

Institut für Immunologie, Friedrich-Loeffler-Institut, D-17493 Greifswald-Insel Riems, Germany

Received December 12, 2018; Revised January 04, 2019; Editorial Decision January 08, 2019; Accepted January 10, 2019

ABSTRACT

Caliciviruses use a termination/reinitiation mechanism for translation of their minor capsid protein VP2. A sequence element of about 80 nucleotides denoted 'termination upstream ribosomal binding site' (TURBS) is crucial for reinitiation. RNA secondary structure probing and computer aided secondary structure prediction revealed a rather low degree of secondary structure determinants for the TURBS of the rabbit hermorrhagic disease virus. Mutation analysis showed that prevention of duplex formation had major impact on the VP2 expression levels. Restoration of complementarity of the respective sequences by reciprocal mutation at least partially restored reinitiating rates. Synthetic TURBS structures preserving only the secondary structure forming sequences and the known short motifs important for TURBS function were found to drive reinitiation when the altered sequence could be predicted to allow establishment of the crucial secondary structures of the TURBS.

INTRODUCTION

The family *Caliciviridae* comprises important pathogens of humans and animals grouped into the genera *Norovirus*, *Sapovirus*, *Lagovirus*, *Vesivirus* and *Nebovirus* (1). In humans, only noroviruses and sapoviruses are found which are responsible for gastrointestinal diseases. Members of all genera are found in animals causing a variety of sometimes fatal syndromes (1). For many caliciviruses, feasible cell culture systems are missing. This is also true for the calicivirus rabbit hemorrhagic disease virus (RHDV), a member of the genus *Lagovirus*, that is the causative agent for rabbit hemorrhagic disease, a fatal illness of domestic and wild rabbits (2,3). RHD was first described in China in 1984 and spread from there to many countries worldwide. In 1995 the virus was accidentally transmitted from an island to the mainland of Australia (4).

Calicivirus particles are nonenveloped and contain a nonsegmented single stranded genomic RNA of positive polarity. It has a length of about 7.5 kb and contains 2–4 functional ORFs depending on the virus genus and species. Within infected cells a subgenomic mRNA (sg mRNA) is found that is 3′ coterminal with the viral genome. Both viral RNAs are polyadenylated at the 3′ end and carry a viral protein VPg that is covalently linked to the RNA 5′ end via a tyrosine residue (1,5–10).

The sg mRNA encompasses two ORFs coding for the major capsid protein VP1 and the smaller minor capsid protein VP2. In vesiviruses, the VP1 coding part of the upstream ORF is preceded by a region coding for the so-called leader protein whereas murine Norovirus sg mRNA encodes a further protein VF1 from the alternative frame ORF4 overlapping the VP1 coding region (1,11,12). VP2 is expressed via a translation termination/reinitiation mechanism from the 3′ terminal ORF that overlaps by a few nucleotides with the preceding VP1 encoding ORF (reviewed in (1)). This reinitiation process is enabled by the so-called 'termination upstream ribosomal binding site' (TURBS), a sequence element of ca. 45 to 80 nucleotides located within the VP1 coding region of the RNA closely upstream of the start/stop site at which termination and reinitiating take place (13–16). The TURBS contains three defined sequence motifs necessary for its function (17,18). Motif 1 is a short sequence containing a pentamer conserved among caliciviruses and also found in TURBS elements from other origins. Motif 1 hybridizes to a complementary sequence in the 18S rRNA of the small ribosomal subunit (17). According to a widely accepted working hypothesis, the interaction of TURBS motif 1 and 18S rRNA helps to keep the terminating ribosome bound to the viral RNA for a certain time to allow reloading of initiation factors necessary for translational restart.

*To whom correspondence should be addressed. Tel: +49 3835 171 0; Email: gregor.meyers@fli.de
Present address: Felix Kreher, MRC-University of Glasgow, Centre for Virus Research, Glasgow, UK.

The other two motifs, named motif 2* and motif 2, are not conserved by primary sequence but by location and the feature that both are complementary to each other (16–18). Thus, motifs 2* and 2 are able to form a stem loop structure that was proposed to be important for presentation of motif 1 and determination of the start site via positioning of the ribosome at or close to the AUG.

Secondary structure elements in RNA are of major importance for the function of these molecules. This is especially important for viral (genomic) RNA for which replication and translation is dependent on structures located at defined positions of the nucleic acid. Extensive stem loop structures and sometimes also pseudoknots are functional features of internal ribosome entry sites promoting translation of viral RNA, and cis-acting elements driving RNA replication (19–28). Pseudoknots also work in programmed ribosomal frameshifting, stop codon readthrough and enzymatically active RNA [see (19,29,30) for review]. The engagement of RNA structural elements in a variety of alternative mechanisms of protein translation suggested a role of secondary structures also in TURBS driven reinitiation. Of course, the complementarity of motifs 2* and 2 indicated already the formation of a stem loop via hybridization of these two sequences. This hypothesis received significant support from work on feline calicivirus (FCV) for which prevention of hybridization via mutation of motif 2*/2 residues drastically reduced reinitiation rates whereas restoration of hybridization via reciprocal exchanges in both motifs (C–G to G–C pairs) increased VP2 expression to about wt level (17). However, this approach did not yield equivalent results for other TURBS elements raising the question about the importance of secondary structure elements for TURBS function. Several groups have conducted (partial) secondary structure probing for different TURBS regions or predicted secondary structure models (15,17,31–34) but so far, a clear structure/function relationship was not determined. In the present report we conducted secondary structure analyses for the RHDV TURBS, mutated putatively hybridizing complementary regions and evaluated the effects of these changes on both VP2 expression and secondary structure. Our analyses defined a very low number of short duplex regions required for reinitiation. This finding was verified by establishment of functional synthetic TURBS structures encompassing only these essential elements embedded at the appropriate positions in a completely altered sequence surrounding, demonstrating that these motives are essential and sufficient to promote termination reinitiation.

MATERIALS AND METHODS

Cells and viruses

BHK-21 cells (kindly provided by T. Rümenapf, Veterinary University Vienna, Austria) were grown in Dulbecco's modified Eagle's medium supplemented with 10% fetal calf serum and nonessential amino acids.

Vaccinia virus MVA-T7 kindly provided by B. Moss (National Institutes of Health, Bethesda, MD, USA) and G. Sutter (Ludwig-Maximilians-Universität, München, Germany) (35,36).

Construction of recombinant plasmids

Restriction and subcloning were done according to standard procedures (37). Restriction and modifying enzymes were purchased from New England Biolabs (Schwalbach, Germany), and Thermo Fisher Scientific (Karlsruhe, Germany).

As a first step for secondary structure analysis, plasmid pBlue-SP6-TURBS was established via insertion of a 139 bp cDNA fragment starting with a SacI site introduced by mutagenesis 123 nt upstream of the start/stop site and ending with the EagI site in the polylinker of pRmRNA (14) into the pBluescript-SK+ vector, followed by insertion of a SP6 promotor sequence into the SacI site and introduction of a EcoRV site 39 nt downstream of the ORF2 start site. Since transcription templated by this construct yielded several bands, construct pStr was established with a smaller cDNA fragment generated by PCR with primers rw4f (GCGGCCGCGATATCATTTAGGTGACACTAT AGAGCTCAACC) rw4r: ATGCATTGCTCAGGGATC CGATATCGGCACCTGCAAGTCCC, and inserted into the BamHI and NotI sites of a modified pBR322. The rw4f primer introduced an EcoRV site upstream of the SP6 promotor, so that the complete cassette can be released with EcoRV prior to in vitro transcription. For mutagenesis, standard PCR based methods with thermostable Pfu polymerase (Promega, Heidelberg, Germany) and synthetic primers purchased from Metabion (München, Germany) were used. The cloned PCR products were all verified by nucleotide sequencing with the BigDye Terminator Cycle Sequencing Kit (PE Applied Biosystems, Weiterstadt, Germany). Further details of the cloning procedure and the sequences of the primers are available on request from the authors.

Expression, detection and quantification of proteins

Transient expression of plasmids in BHK-21 cells using vaccinia virus MVA-T7, metabolic labelling with Tran^{35}S-Label, cysteine [^{35}S]cysteine or [^{35}S]methionine (ICN-MP Biochemicals, Eschwege, Germany or Hartmann Analytic, Göttingen, Germany), preparation of cell extracts and recovery of immunoprecipitates with double precipitation were done as described (14). Briefly, VP2 expression efficiency was quantified after SDS-PAGE separation of VP1 and VP2 precipitated with antisera 'antiRHDV-M' and 'antiRHDV-N', respectively (38). Double precipitation was used to assure quantitative recovery of the proteins as tested before (14). The precipitates were combined and aliquots thereof separated by 10% PAGE using the gel system published by (39). The gels were analyzed with a Fujifilm BAS-1500 or a CR-35 Bio image plate scanner, and intensities of the signals were determined with TINA 2.0 or AIDA Image Analyser 5 software (equipment and software from Elysia-Raytest, Straubenhardt, Germany). The molar ratio of VP1 and VP2 was calculated based on the number of labelled residues within the proteins and the measured radioactivity. For comparison of expression efficiencies of different constructs, the VP2 expression levels of the wt construct pRmRNA was defined as 100%. The amount of VP2 expression of the other constructs was normalized to the values determined for VP1 as internal standard. The corrected value for

VP2 was then used for calculation of the expression efficiency given as percentage of the wt value. The data presented here represent the averages of at least 4 independent experiments. Statistical analysis in form of a two-tailed T test was done using the GraphPad Prism software (Statcon GmbH, Witzenhausen, Germany).

Structure probing

For *in vitro* transcription, the EcoRV fragment of pStr containing SP6 promotor and the RHDV TURBS sequence was purified via agarose gel electrophoresis. The DNA was isolated from the gel with the NucleoSpin GelExtraction kit (Macherey and Nagel, Düren, Germany) and used as template for transcription with the RiboMAX Large Scale RNA Production System (Promega, Heidelberg, Germany). DNA template was degraded via DNase as recommended and the RNA purified on a Sephadex G50 spun column (Sephadex G50 DNA grade, GE Healthcare, Fisher Scientific, Schwerte, Germany) (37). For 5′ end labeling, 10 μg of RNA were dephosphorylated with 50 units of Antarctic Phospatase for 90 min as recommended (New England Biolabs). The enzyme was heat inactivated at 70°C for 15 min, and the mix was cleaned by passage through a Sephadex G50 spin column.

The dephosphorylated RNA was labelled at the 5′ end for 1 h at 37°C with 50 μCi γ-^{32}P-ATP (ICN-MP Biochemicals or Hartmann Analytic) and T4 polynucleotide kinase (New England Biolabs). Residual free nucleotides were removed by passage through a Sephadex G50 spun column. The eluate was purified by phenol/chloroform extraction and precipitation of RNA with 2.5 times the volume of ethanol.

The redisolved RNA was further cleaned by electrophoresis through a denaturing preparative 8% acrylamide/8M urea gel (37). The product band was cut out from the gel visualized in UV light with the help of a thin layer chromatography plate, the RNA eluted by diffusion into 400 μl of 0.5% SDS at 40°C for 48–60 h and the resulting solution extracted with phenol/chloroform and the RNA precipitated with ethanol in the presence of 50 μg of yeast tRNA. The product was dissolved to 500–1000 cps/μl (measured in a Mini Assay type 6–20 counter, Mini Instruments LTD, Essex, UK).

To obtain a ladder in one nucleotide steps as a control for electrophoresis, 2 μl of the radioactively labeled RNA were diluted with 13 μl of alkaline hydrolysis buffer (Ambion/Thermo-Fisher, Schwerte, Germany), devided into three aliquots, and incubated for 4, 5 and 6 min at 95°C followed by chilling on ice and addition of 10 μl gel loading buffer II (Ambion).

For secondary structure analysis, end-labelled RNA was treated with RNase A (cleavage after ss pyrimidine residues), RNase T1 (cleavage after ss G), nuclease S1 (cleavage of single stranded residues) or RNase V1 (cleavage of base-paired regions) (all enzymes from Ambion). All RNases were provided by the supplier together with 10× structure buffer, 1× sequencing buffer; alkaline hydrolysis buffer, inactivation/precipitation buffer and gel loading buffer. For each RNase 0.2–3 μg of labelled RNA were mixed with 3 μg of yeast tRNA and 10× structure buffer or 1× sequencing buffer to a final volume of 27 μl. The reaction mix was split into three tubes and 1 μl of the specific RNase was added to the first tube. The enzyme was consecutively diluted by transferring 1 μl of the mixture in tube 1 to the second and from the second one again 1 μl to the third tube. Amounts of nuclease added to first tube: 1 U RNase T1; 50 ng RNaseA; 10 U S1-nuclease; 1 ul (0.1 mU) nuclease V1. The digestion was done for 5 min at 37°C and stopped thereafter by adding 20 μl of inactivation/precipitation buffer. For the T1 sequencing reaction, a denatured RNA was produced by incubation of the labelled RNA at 55°C for 5 min followed by chilling on ice. The treatment with the T1 RNase was conducted as described above and stopped as described there. The reaction mixtures were incubated on ice for 20 min and the precipitated RNA collected by centrifugation (30 min at 4°C and 20 800 × g), dried, dissolved in 7 μl gel loading buffer II and separated on urea acrylamide sequencing gels (37).

Sequence analysis and structure prediction

Basic sequence analysis was conducted with the Geneious 10 software package (Biomatters, Aukland, New Zealand). Secondary structure prediction of RNA sequences was done with the RNAstructure software of the Mathews lab, Department of Biochemistry & Biophysics, University of Rochester Medical Center, Rochester, New York 14642, USA using the settings of the system (https://rna.urmc.rochester.edu/RNAstructure.html).

RESULTS

Secondary structure elements of the RHDV TURBS

The so far published analyses leading to identification of the RHDV TURBS were conducted with the cDNA construct pRmRNA (Figure 1), from which an RNA resembling the sg mRNA of the virus can be transcribed, in which the 84 3′-terminal residues of ORF1 represent the TURBS that drives translation of ORF2 via a termination/reinitiation mechanism (14,18). Similar arrangements were also found for other viruses using this type of translation initiation (13,15,16,32,40). The 84 residues were sufficient to induce reinitiation, and, therefore, have to contain all necessary primary and secondary structure elements of the TURBS (14,18). Computer assisted secondary structure prediction was performed for a ∼100 nucleotide sequence encompassing these 84 nucleotides plus some upstream residues using the RNA structure software of the Mathews lab, University of Rochester, USA (https://rna.urmc.rochester.edu/RNAstructure.html). The two structures with the highest ΔG values differed only in a central part where the motif 1 sequence known to hybridize to 18S rRNA (17) was partially double stranded in one structure but single stranded in the other (Supplementary Figure S1). The latter structure was predicted as the most likely one according to the MaxExpect analysis (RNA structure software of the Mathews lab, University of Rochester).

To get more information on the secondary structure of the TURBS region we conducted structure probing experiments in order to identify base paired and single stranded nucleotides of a folded RNA in a differentiating way. Most of the analyses were done with limited nuclease digestion of

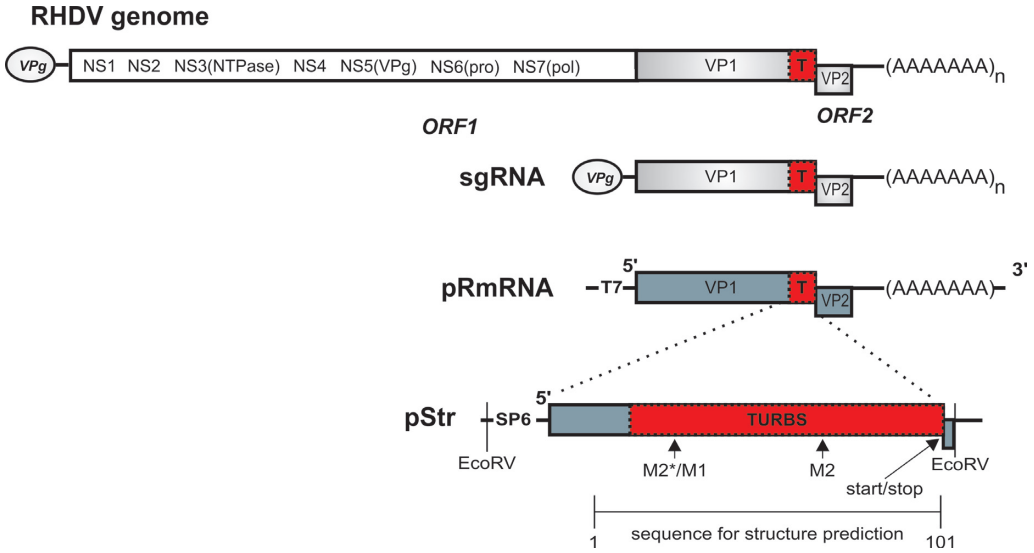

Figure 1. Schematic representation of the RHDV genomic and subgenomic RNA organization and important features of the cDNA constructs pRmRNA and pStr. The RHDV genome is shown on top with the location of the different protein coding regions. All nonstructural proteins as well as the major capsid protein VP1 are encoded in one long open reading frame (ORF1) whereas ORF2 encodes only the minor capsid protein VP2. Below, the subgenomic RNA is depicted, which is 3′ coterminal with the genome and codes for the structural proteins. Both genome and subgenome (sg) carry a covalently bound VPg protein at the 5′ end and a poly(A) tail at the 3′ end. The 3′ terminal region of ORF1 contains the TURBS (T) highlighted in red. Below the RNA schemes, the cDNA construct pRmRNA is shown from which an RNA similar to the sgRNA can be transcribed (14). At the bottom, construct pStr is indicated as a blow up. This plasmid served as a template for transcription of the RNA used for structure probing.

5′-end labeled RNA transcribed from construct pStr (Figure 1), which encompasses the complete TURBS region and flanking sequences. This RNA contains 113 residues upstream of the start/stop site, the site itself and 29 nucleotides downstream thereof as well as 5 non-RHDV residues (in total 155 N) together with a SP6 promoter for *in vitro* transcription. The transcribed RNA was dephosphorylated, 5′ end labeled with 32P γ-ATP and subsequently purified by preparative PAGE in a denaturing gel to get rid of truncated RNA. The product eluted from the gel served as starting material for structure probing.

We used the RNases T1 (specific for single stranded G residues), A (specific for single stranded C and U) and V1 (cleaves on the 5′ side of double stranded nucleotides). In addition, nuclease S1 was used which cleaves 5′ of single stranded residues without base specificity. Two different reactions were conducted with RNase T1, one with completely denatured RNA resulting in bands for any of the G residues present in the RNA (Figure 2, reaction T1 Seq) while the second was run under native conditions so that only unpaired G residues should result in a band (reaction T1). To obtain folded RNA for structure analysis reactions, the reaction mix without enzymes was heated to 55°C for 5 min and then slowly cooled down to room temperature before nucleases were added. Reactions were conducted with different dilutions of the enzymes. A sample without enzyme served as a control for identification of nonenzymatic degradation of the RNA. As a further control, one lane was loaded with a sample of the 5′ end labeled starting material without further treatment or incubation to identify bands already present before starting the reactions (lane '0'). To be able to identify the sequence position corresponding to individual bands the products of a limited alkaline hydrolysis were run next to the lanes with the structure probing samples (lane 'ladder'). The resulting ladder together with the T1Seq lane allowed precise identification of the bands detected via the structure probing.

The starting material contained one predominant band representing the desired labeled RNA and a lower amount of a smaller product (marked with an asterisk in Figure 2A). These two RNA species could not be separated from the full length RNA fragment during the purification procedure because of their very similar molecular weight. However, due to its much lower abundance this contaminating smaller RNA did not negatively influence the results of the analyses.

Treatment of the denatured or natively folded RNA with the different nucleases yielded characteristic and reproducible cleavage profiles. Most of the G residues were found to be accessible for RNase T1 in both denatured and native RNA (compare lanes T1Seq and T1 in Figure 2). Similarly, RNase A and nuclease S1 treatment resulted in multiple band profiles. It has to be stressed that nuclease S1 did not seem to cleave at all single stranded nucleotides as can be concluded from a comparison of the S1 lane with the T1 and A lanes in Figure 2. Taken together, the analyses showed that the TURBS is a rather unstructured RNA element. The partial overlap of signals obtained with single strand specific nucleases and with the double strand specific V1 RNase is most likely due to the fact that the latter nuclease can also cleave single stranded nucleotides with stacked bases.

Most of the motif 1 residues (GUGGGA, 26–32 in Figure 2B) were found to be single stranded. Only the A at the 3′ end gave no interpretable signal. This result was expected since motif 1 has to be single stranded to allow hybridization with its counterpart in the 18 S rRNA (17). In contrast, the motif 2* and 2 regions were found to contain paired residues, which is in accordance with mutagenesis

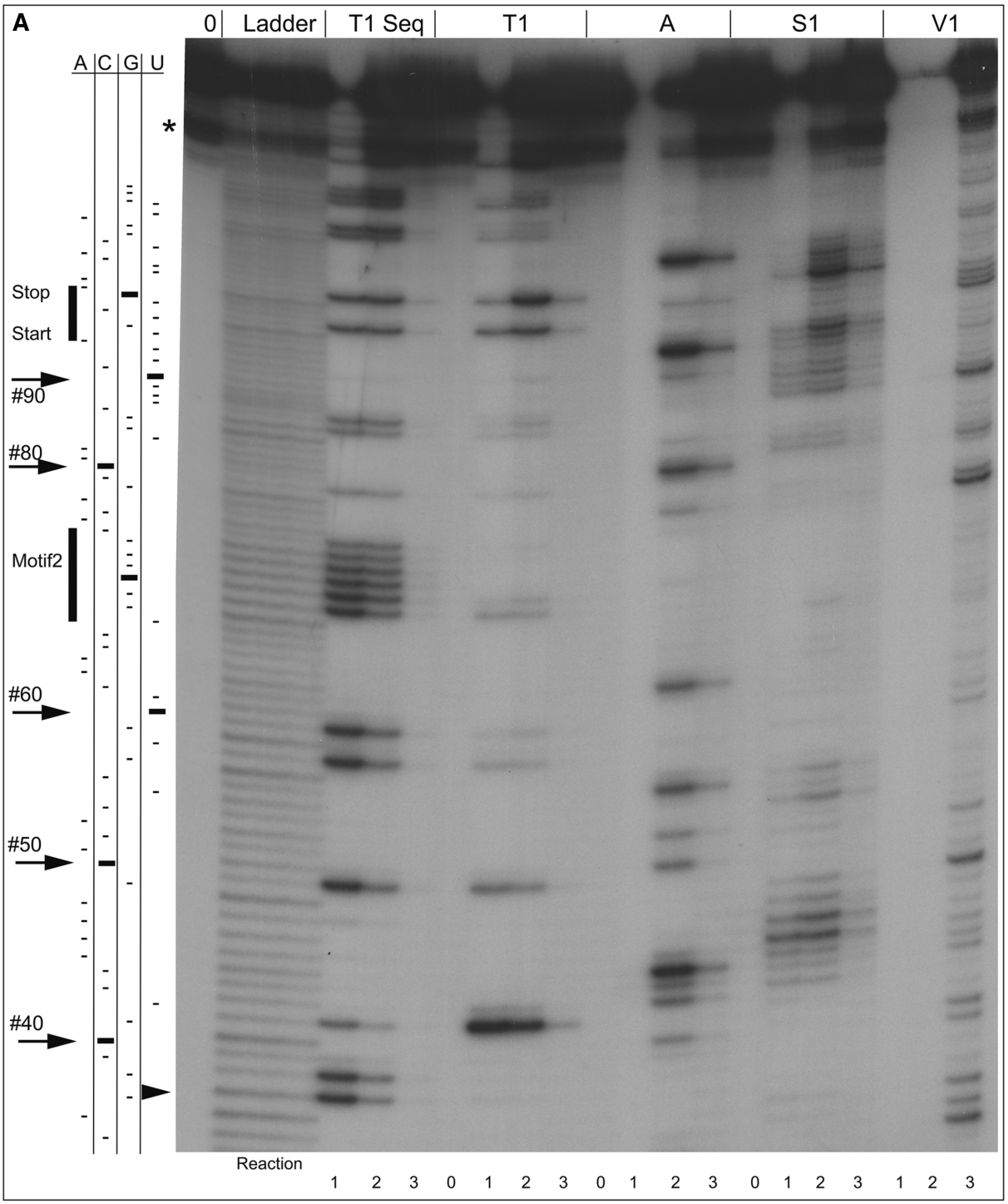
A
0
Ladder
T1 Seq
T1
A
S1
V1
A C G U
*
Stop
Start
#90
#80
Motif2
#60
#50
#40
Reaction
1 2 3 0 1 2 3 0 1 2 3 0 1 2 3 1 2 3

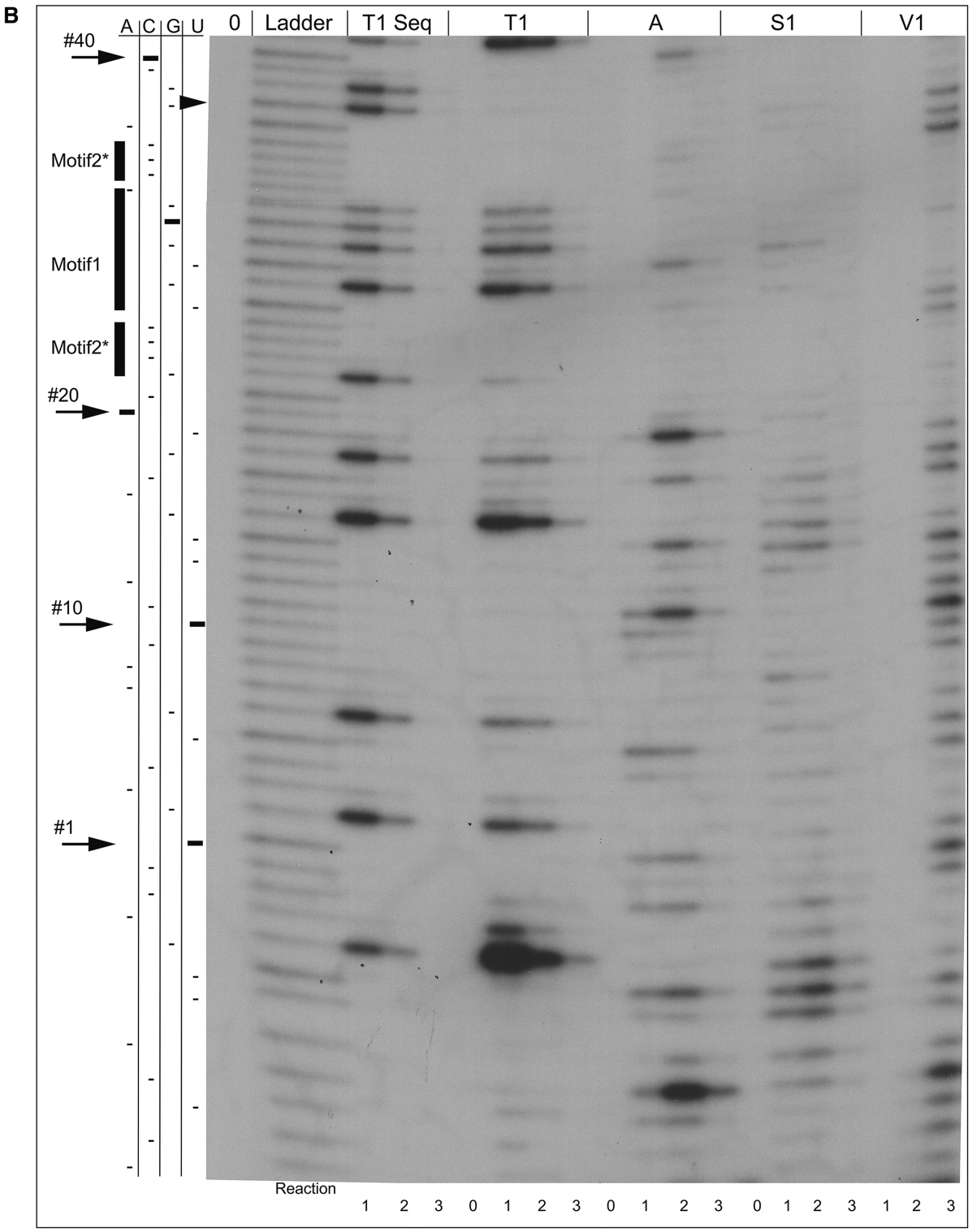

Figure 2. Enzymatic secondary structure probing results. 5′ end labelled RNA transcribed from a pStr derived cDNA fragment (Figure 1) was subjected to limited digestion with the indicated enzymes (T1 = RNase T1, bands in T1 lane result from single stranded G; A = RNase A, bands result from single stranded C and U; S1 = nuclease S1, bands result from single stranded nucleotides; V1 = nuclease V1, bands result from double stranded or stacked residues). The ladder was obtained by loading a sample of the test RNA subjected to limited alkaline hydrolysis. Lane T1 Seq shows the results of limited digestion of denatured test RNA, whereas lane T1 contains the products of the same treatment but with folded test RNA. Below the gels, numbers indicate the different dilutions of the enzymes used for the respective reaction (dilutions increase with numbers). On the left side of the gels, the sequence of the RNA is shown as a banding pattern. In addition the location of motif 1, motif 2* and motif 2 is indicated. Numbering refers to the sequence shown in Figure 3. The gel is shown in two parts with (A) and (B) representing the upper and lower parts, respectively. An arrowhead marks an identical position on both gels for better orientation.

studies demonstrating the importance of the complementarity of these sequences which is conserved among different TURBS elements (17). Strong evidence for paired nucleotides was found within the region of positions 35–38 (CAGG) (see also Supplementary Figure S2), G 57 and G 59 (unclear for U 58), and 84–85. Some evidence for double strands was found for residues 16–18 (RNase A cleaved but no S1 signal for several residues and bands in V1 lane). Strong indication for base pairing was also found for residues downstream of the relevant TURBS region, namely the GG and GGG stretches in the sequence from 109 to 116 (significant reduction of the G bands in the T1 lane compared to T1Seq lane) whereas other nucleotides within this region (111–113) gave no clear results.

For further support of the RNA secondary structure data obtained after RNase treatment we conducted analyses based on chemical treatment of the transcribed RNA and subsequent primer extension cDNA synthesis. These analyses rely on preferential chemical modification of specific unpaired bases and the feature of the reverse transcriptase to stop synthesis at these modified bases. The theoretical advantage of the chemical treatment is the reduced sterical hindrance for the access of the small chemical compounds compared to the much larger enzymes. All primer extension reactions of the TURBS RNA produced a high background that could not be controlled by adjustment of the protocol (Supplementary Figure S2). This background problem was specific for the TURBS RNA since a control with an unrelated sequence did not show similar background (not shown). For a number of nucleotides the results were not interpretable since bands were obtained for both AC or GU specific treatments (DMS or CMCT, respectively), single strand (Pb^{2+}) as well as double strand (V1) detecting reactions, often with signals in all lanes. Nevertheless, interpretable results were obtained for a significant number of residues and summarized in a simple way in Figure 3 together with the data generated via the enzymatic analyses. The presentation of the results in Figure 3 is based on one of the predicted folds (Supplementary Figure S1) that provided the best match with the experimental data. This was especially true for the sequences flanking motif 1 which include the predicted motif 2*/2 interaction. Obvious deviations were found for the first and last ∼20 nucleotides for which the probing gave mainly contradictory results with bands in the V1 lane as well as lanes specific for single stranded residues. For part of the residues we did not obtain the desired information from the probing because bands were either not detected at all or visible both in lanes indicating paired and single stranded RNA. The latter can result from stacking of bases in tertiary structure that can also force the RNA to adapt a specific secondary structure (41). Importantly, almost all residues found double stranded in the probing experiments were also paired in the predicted model.

Verification of the putative double strand interactions in the motif 2*/2 context by mutagenesis

Only a rather limited number of nucleotides were found to be paired by probing as well as prediction. The predicted structure based on minimizing the free energy possessed some additional paired regions that could not be fully supported experimentally. In order to determine which of the proposed paired regions are important for TURBS function, mutagenesis analyses were conducted. The residues to be mutated were selected in accordance to the structure model shown in Figure 3.

The significance and functional importance of the motif 2*/2 interaction was already demonstrated in earlier mutation analyses with the FCV TURBS (17) and also the results obtained in experiments with the RHDV TURBS supported this conclusion (18,34). In FCV, motif 2* is located as a continuous sequence upstream of motif 1. A similar configuration is also found in the RHDV TURBS with nucleotides GCCC (putative motif 2*, position 22–25) preceding motif 1 and GGGC representing a likely motif 2 (position 71–74). However, although not fully supported by the probing data (Figure 3), the sequence downstream of motif 1 (CCCAGG, positions 33–38) should hybridize with the CCUGGG sequence (positions 65–70) preceding the above mentioned putative motif 2 sequence GGGC. To analyze whether functional aspects supported the interaction predicted for the motif 2*/2 region the VP2 expression of constructs with nucleotide exchanges in either part of putatively paired sequences was determined. As a second step, the reinitiation rate of double mutants, in which the possibility for pairing was restored because of reciprocal exchanges on both sides, was tested after transient expression and quantitative immunoprecipitation followed by autoradiography scanner quantification of VP1 and VP2 as described before (14) (Figure 4).

The predicted stem preceding motif 1 is in accordance with published data (15–17,32,34), and supported by our structure probing results. Exchanges of the respective residues dramatically affected VP2 expression. Both the exchange of 3 nucleotides of the left and right part of the paired sequence resulted in reduction of VP2 expression to almost 0 (constructs p1A and p1B, respectively). The functional importance of duplex formation was further supported by the partially restored VP2 expression level of construct p1AB that contains the reciprocal exchanges on both sides (Figure 4A). The rather low expression level of p1AB of only 19% can result from formation of quite stable secondary structures ($\Delta G < -30$ kcal/mol) predicted by Mfold that contain a paired motif 1 (UGUGGG paired, data not shown). According to our model, pairing of motif 1 would unequivocally interfere with TURBS function.

We also tested variants, with exchanges affecting both stems flanking motif 1 resulting in a total loss of three C–G pairs (p2A) as well as mutant p2B that contains the p2A exchanges together with two reciprocal alterations and a further exchange resulting in loss of only one pairing in each stem. The VP2 expression of p2A was reduced to 1.6% whereas mutant p2B showed 25% of the wt levels (Figure 4A).

As already mentioned above, the predicted interaction of the sequence downstream of the motif 1 with the two first Gs of motif 2 was only indicated by the reduced intensity of the bands whereas the other 4 G's were identified as paired in the T1 analysis. Total prevention of hybridization via exchange of all 6 predicted paired G residues in construct p3_4 abrogated VP2 expression almost completely (3% residual

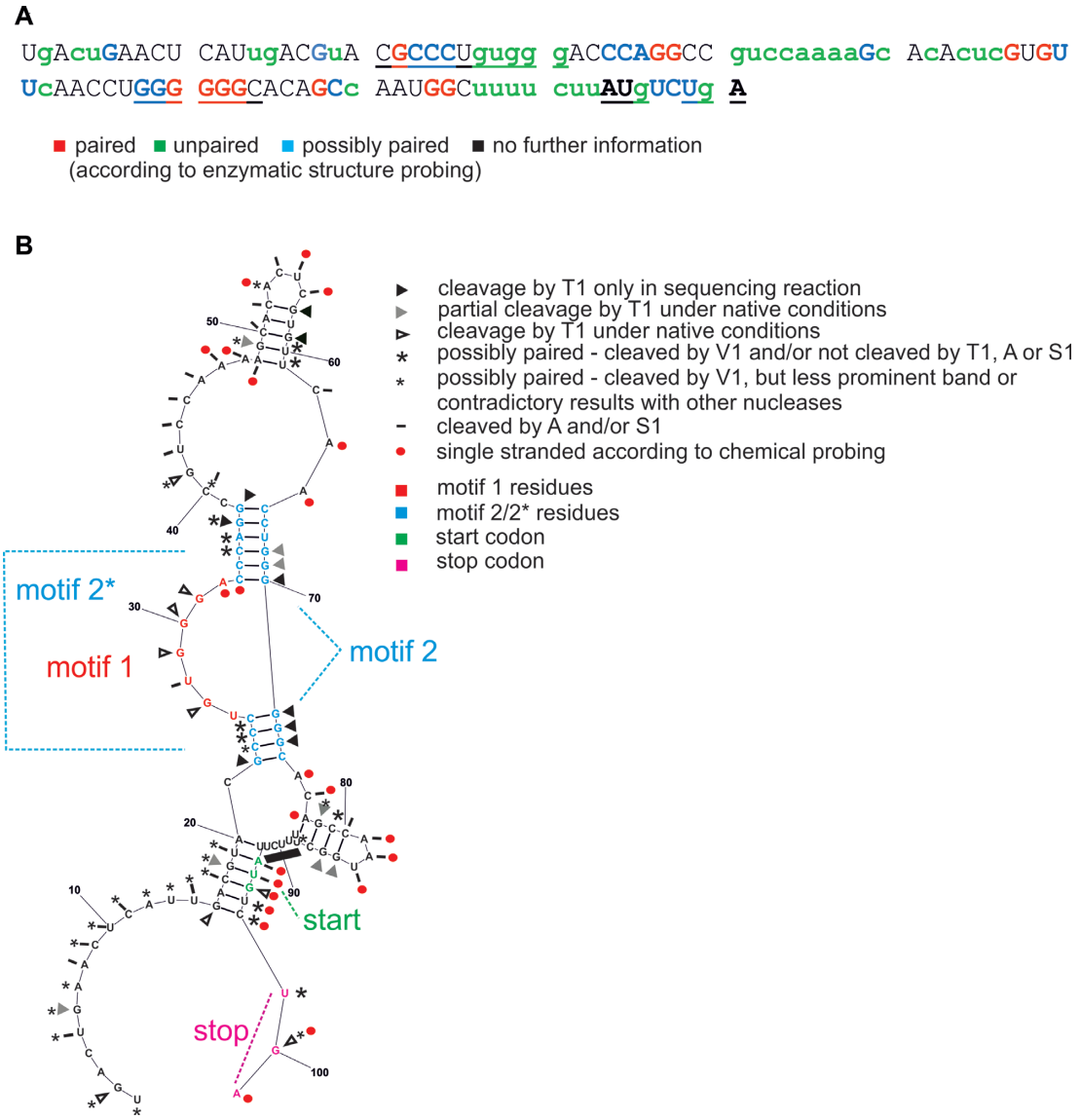

Figure 3. Summary of secondary structure probing results. (**A**) The TURBS sequence is shown in form of a text with a colour code indicating the main results of the enzymatic structure probing shown in Figure 2 (colour code given below the text). For better differentiation, nucleotides found to be single stranded are given in lower case. Residues for which contradictory or no results were obtained are referred to as 'no further information'. (**B**) The results are included in a predicted secondary structure (Supplementary Figure S1, right part). Nucleotides, for which no further information could be deduced from the structure probing are without label whereas the other are marked according to the given code. The results deduced from all bands of considerable intensity in Figure 2 are shown. Due to the background obtained after chemical probing (Supplementary Figure S2) only results from bands showing a significantly higher intensity than the bands in neighbouring lanes are included. The black bar found around position 90 indicates that all these nucleotides were found single stranded in the probing (cleaved by RNase A and/or nuclease S1). The motif 1 nucleotides are given in red and the experimentally proven motif 2*/2 sequence is shown in blue.

activity, Figure 4b). The same effect could also be observed when only the lower triplet of the stem downstream of motif 1 was changed [constructs p3A and p3B with 3 and 2% of wt expression levels, respectively (right part of Figure 4B)]. Combination of both mutations in p3AB restored the pairing possibility and resulted in ca. 43% of wt levels of VP2 expression, which strongly supports the conclusion that these residues have to form a duplex to allow efficient reinitiation (Figure 4B).

In a next step, we tested the importance of 3 paired residues in the upper half of the six residue stem downstream of motif 1. The reinitiation efficiency for the different exchanges affecting the 2 G-C pairs is reduced to 45, 26 and 56% in constructs p4A, p4B and p4C, respectively (left part of Figure 4B). A reciprocal change at these positions of the stem in plasmid p4BC changing G–C to C–G pairs restored the VP2 wt expression levels almost completely (88% of wt). Exchange of all three upper residues on either site reduced reinitiation efficiency to 19% (Figure 4, constructs p4D and p4E). Changing both sides of the putative duplex to obtain complementarity again partially restored VP2 levels to 44% of wt (p4DE, middle part of Figure 4B). The lower level of

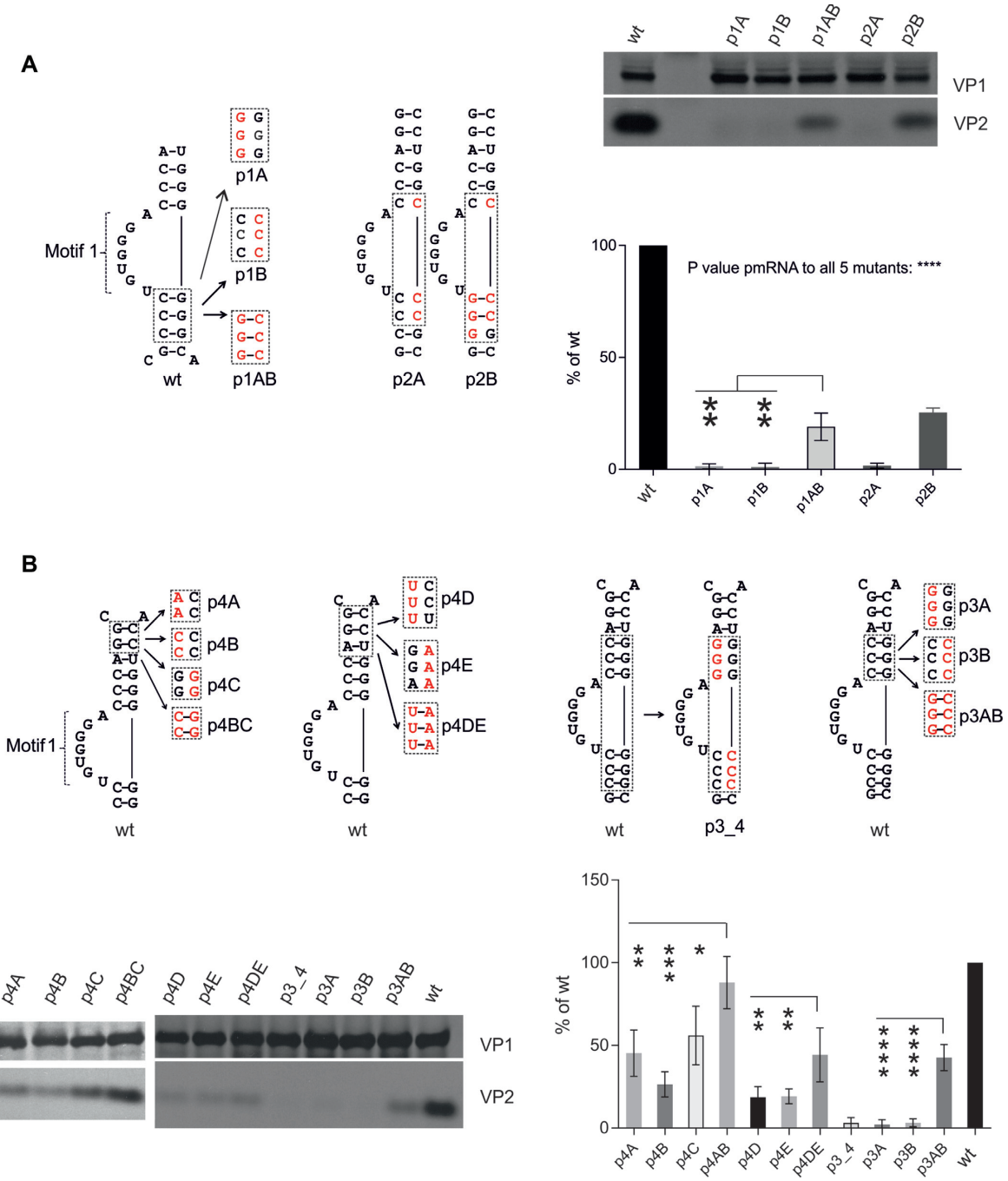

Figure 4. Mutation analysis of the proposed stem sequences flanking the motif 1 region in the predicted TURBS structure. On top, the analysed part of the structure predicted for the wt and the sequences of the different mutants are shown with exchanged residues given in red. Below, the results of quantitative immunoprecipitation of VP1 and VP2 transiently expressed from the indicated constructs are represented. The bar diagrams summarize the results of at least four independent expression experiments with the bars giving the VP2 expression levels as per cent of the wt levels. The VP2 expression was normalized for each construct to the amount of VP1 and thus reflects the rate of reinitiation in comparison to the wt sequence. Error bars are indicated. Asterisks represent the *P* values (**P* < 0.05; ***P* < 0.01; ****P* < 0.001; *****P* < 0.0001). (**A**) mutations affecting (mostly) the stem preceding motif1, (**B**) mutation affecting the stem following motif 1 or equally both stems.

reinitiation restoration observed here could be due to the lower stability of two U-A instead of two G–C pairs.

Taken together, the results of the mutagenesis analysis strongly support the conclusion that the RHDV RNA folds in a way that the single stranded motif 1 is flanked by two stem structures of four and six paired nucleotides, respectively. These structural elements are functionally important and most of the respective residues were identified as paired in the probing experiments.

Functional importance of other predicted secondary structures

In contrast to the motif 2*/2 interaction, for which functional importance had to be expected due to earlier studies (17,18,40), three further paired elements are found in the predicted structure, with rather limited support from the structure probing results (Figure 3). In a further mutagenesis approach we analyzed the possible functional importance of these putative strutures. The stemloop composed of residues 48–61 (top stem–loop) is found in different structure predictions. We did not find indications for duplex formation for the left side of the proposed stem but the GUGUU motif on the right hand side was identified as double stranded (Figure 3). Exchange of ACU for GUG (p5A) or CACA for the GUGU (p5B) had only very limited impact on VP2 expression (Figure 5). Deletion of the entire top stemloop except for the first and last residue reduced VP2 expression to 48% of wt levels (construct p5C, Figure 5). A similar level (46%) was obtained when 12 additional residues were deleted in construct p5D. These findings strongly suggest that the top stemloop with its flanking regions has no major functional importance, and, in a more general view, the pairing of the GUGU motif is not crucial for TURBS driven reinitiation.

A second stemloop was predicted for residues 77 to 87, closely upstream of the start/stop region. Again, the sequences of this predicted double stranded sequence (5′ part AGCC, 3′ part GGCU) were only partially identified as duplex via structure probing. Replacement of the GCC in the upstream part of the stem (construct p6A) and the GG in the downstream moiety (constructs p6B and p6C, Figure 5) resulted in a residual VP2 expression efficiency of at least 84% of wt levels, showing that this putative secondary structure element is not relevant for TURBS function.

The third so far not further analyzed region for which double strands were predicted by MFold consists of residues 15–20 and 93–98. The structure probing resulted in contradictory data or single stranded RNA for these residues. Earlier analyses conducted for the start/stop region with exchanges affecting the UC residues located between start and stop codon as well as replacement of the UGA stop codon by UAG or UAA had revealed significantly reduced reinitiation efficiency to 48–36% of wt level (14). We therefore tested a further set of mutants with GA 15/16 replaced by CU (construct p7A) or UC between start and stop codon by AG (positions 97/98, construct p7B), and a construct with both of these changes that should restore the proposed pairing (p7AB). Transient expression experiments resulted in VP2 expression levels of 75% for p7B, 89% for p7A and 115% for p7AB (Figure 5) which shows that also this putative interaction is not of major importance for reinitiation. This conclusion is supported by the fact that residues 93 to 98 would be occupied by the ribosome during reinitiation.

A variety of different structure predictions can be obtained for the 3′ end of the TURBS including the start/stop region. In one interesting example, the GGC (84–86) identified as paired in the probing experiments forms a duplex with the G of the AUG and the UC located between start and stop codon. However, it has to be stressed that both Gs of the AUGUCUGA start/stop are clearly single stranded in the structure probing. Moreover, mutations affecting the above mentioned GGC as in constructs p6B or p6C had no drastic effect on VP2 expression (Figure 5). Taken together, clear evidence for the structure of the start/stop region is still missing at the moment. It has to be questioned whether the moderate effects of base exchanges in this region on VP2 expression efficiency represent a consequence of structural changes or are due to primary effects of sequence alteration. Importantly, it has to be noted that the sequence of this area is not crucial for TURBS function as long as start and stop codons and their respective positioning are preserved.

TURBS elements with grossly changed sequences

The above described analyses showed that the RHDV TURBS contains only a limited number of secondary structure elements that, in addition to the formerly described motif 1 and the start/stop region, could be engaged in translational reinitiation. The mutation analyses indicated a restriction of the crucial structural elements to the motif 2*/2 interaction, whereas alterations of other elements showed only small effects. To demonstrate that the set of motif 1, motif 2, motif 2*, start/stop region, and the correct spacer length between motif 2 and the start/stop region (18) are sufficient for driving reinitiation, we tested TURBS elements with grossly changed sequences for parts of the TURBS that were not identified as crucial for reinitiation. These new sequences should, hopefully, not interfere with establishment of the crucial secondary structures and should not pair with each other. We changed G and U residues in the respective sequences to A and C (Figure 6). Construct p8A contained not only the M1, M2 and M2* sequences but also the paired parts of the putative top and start/stop site loops. In plasmid p8B the top stem loop was eliminated by changing the putative stem sequences together with almost the entire sequence located between the end of motif 2* and the 5′ end of motif 2. Moreover, the GCC and GGC of the start/stop site stem loop were replaced by nonpairing sequences. These constructs induced VP2 expression at ∼40% of wt levels. As mentioned above, the top stemloop was dispensable for reinitiation in the wt TURBS context. We therefore created a further synthetic TURBS with elimination of major parts of the top stemloop region resulting in construct p8C, from which VP2 was expressed with 30% of wt levels.

The idea of the above described approach was to demonstrate that the presence and arrangement of the identified essential motifs of the TURBS is functional even in a different context of surrounding sequences. To verify that the complementarity of the critical sequences is still of key importance in the new context, we introduced several changes

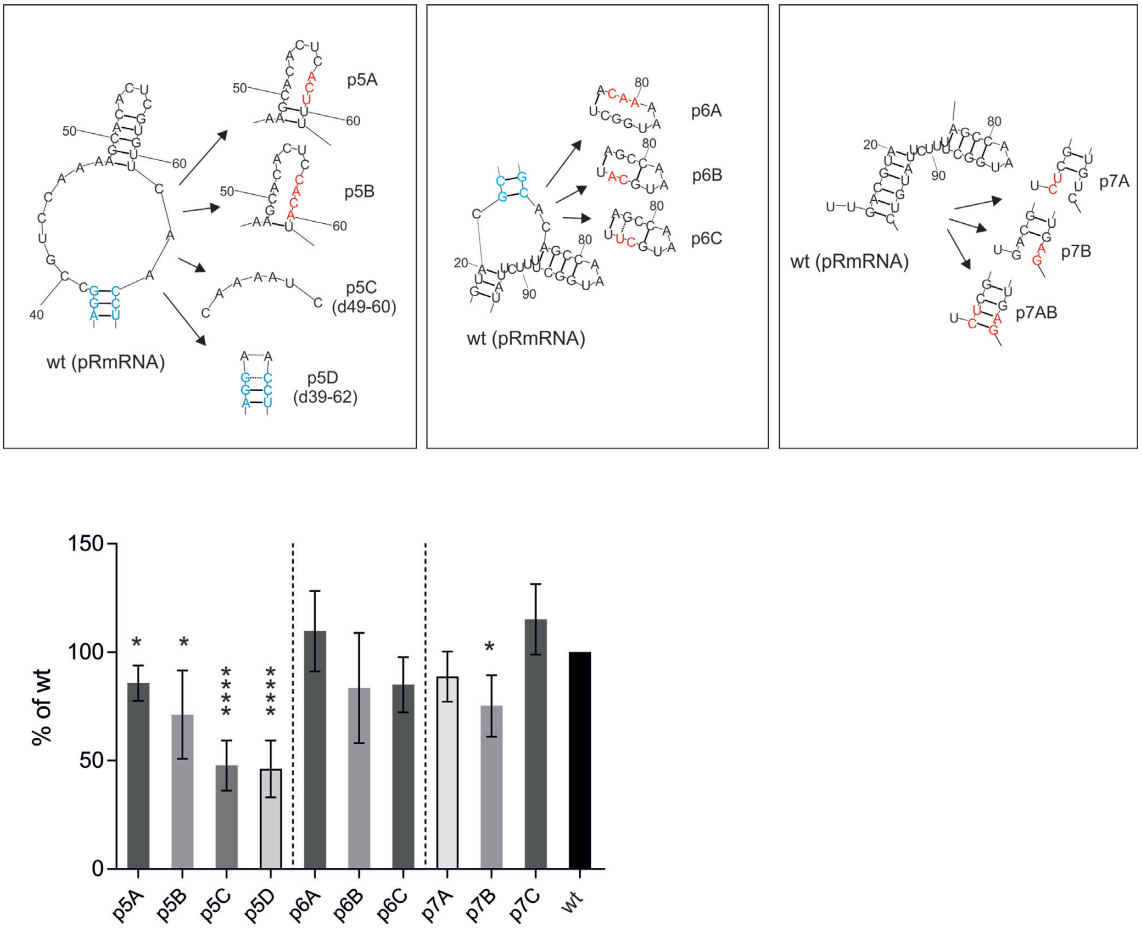

Figure 5. Importance of further predicted secondary structure elements for reinitiation. On top, the predicted structural elements are shown for the wt and the sequences of the different mutants are given with mutated residues shown in red and residues belonging to motifs 2*/2 given in blue. The bar diagram below summarizes the results of at least four independent expression experiments. The VP2 expression levels normalized to the amount of VP1 determined for each construct are presented as per cent of the wt levels with error bars indicated. Asterisks represent P values for differences with regard to wt (*$P <$ 0.05; ****$P < 0.0001$).

into p8C affecting the motif 2*/2 interactions (constructs p8C1, p8C2, p8C3, p8C4, p8C5 and p8C6) (Figure 6). In all cases, a significant reduction of the VP2 expression level was observed with the more elaborate changes having a more pronounced effect. The most prominent reduction of VP2 expression was observed for p8C6 with 8 pairings eliminated. Thus, the possibility to establish motif 2*/2 stems flanking motif 1 is also crucial for reinitiation in the synthetic TURBS.

Analysis of our newly designed TURBS sequences with the secondary structure prediction software resulted in models with motif 1 sequences paired with upstream sequences (see predicted structure of p8B in Figure 6). We therefore created in silico a variety of synthetic TURBS sequence variants and tested them in structure prediction analyses. Construct p8D was predicted to establish a secondary structure equivalent to the original TURBS with the essential motif 2*/2 pairing and a single stranded motif 1 (Figure 6), and showed efficient VP2 expression of 73% of the wt levels. These results provide further support for our structural model and the proposed structure/function relationship.

DISCUSSION

Viruses rely entirely on the host cellular translation machinery since with the exception of a group of exotic viruses (42) they have no components of a translation system. Therefore, viral mRNAs need to compete against a large number of host mRNAs for the limited translation capacity while the viral life cycle often demands large quantities of viral proteins to be produced at specific times. At least in RNA and small DNA viruses, a further problem arises from the limited length of the viral genomes restricting coding capacity and the possibility to establish elaborate signals for regulation of gene expression. In consequence, a variety of alternative translation strategies evolved in viruses [see (19,43) for review], which often rely on special RNA structures like internal ribosome entry sites (IRES) that are able to orchestrate all steps required for translation initiation or somewhat less complex RNA structures responsible for ribosomal frameshifting or translational readthrough at stop codons (19).

Reinitiation after translation of a long ORF is an unusual mechanism of gene expression found in caliciviruses and some other RNA viruses which relies on TURBS ele-

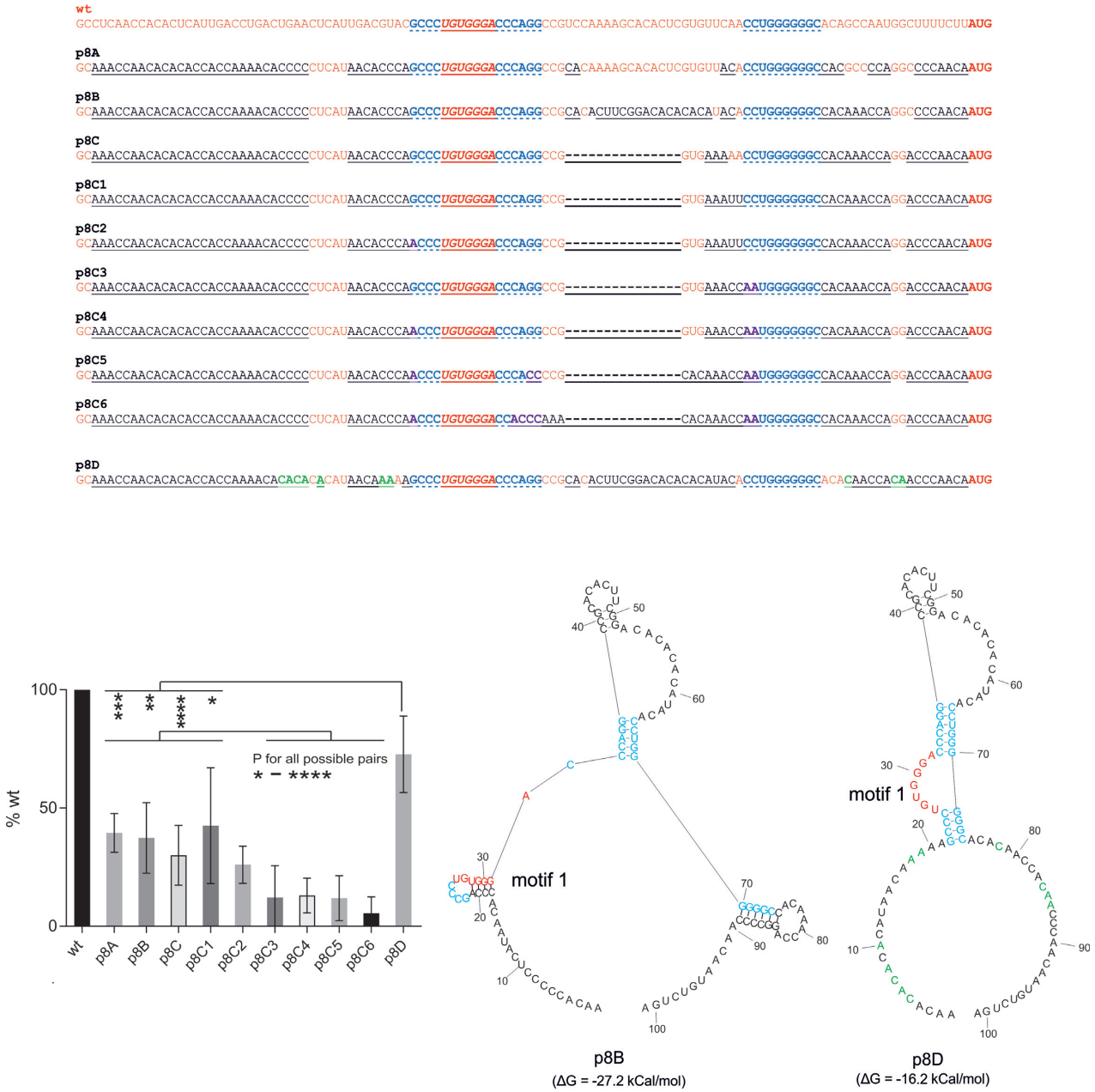

Figure 6. Functionality of grossly altered TURBS sequences. The upper part shows the sequences of the wt construct and the different mutants. The motif 1 sequence and the start codon of the VP2 coding ORF2 are shown in bold red letters with motif 1 underlined, whereas motif 2/2* residues are given in blue with dotted underline. The rest of the wt sequence is shown in red. Sequences differing from the wt are shown in black and underlined or in purple and bold, when the changes affect the known motifs. For p8D, residues differing from p8B are represented by green letters. The bar diagram in the middle shows the VP2 expression levels of these constructs reflecting the reinitation rate given as the percentage of the wt levels. Asterisks represent P values showing the significance of the differences in VP2 expression between the results for p8D in comparison to p8A, p8B, p8C and p8 C1. The latter 4 gave all significantly higher VP2 expression levels than p8C2, p8C3, p8C4, p8C5 and p8C6 as indicated by the p values (*$P < 0.05$; **$P < 0.01$; ***$P < 0.001$; ****$P < 0.0001$). All results except for the one obtained for p8D were significantly lower than the wt value. The bottom part shows the secondary structures predicted for p8B and p8D. The location of motif 1 (red letters) and motif 2*/2 (blue letters) are indicated.

ments. (13,15–18,31–34,40). The TURBS has no (cryptic) IRES activity and thus is only able to either recycle a 40S ribosomal subunit after termination or a post termination 80S ribosome in a specific way (34). Due to the experimentally proven necessity of the motif 1 complementarity to a sequence in the 18S rRNA (17) and the knowledge that regular translation initiation is only possible for an initiation complex containing RNA, the small ribosomal subunit and a set of initiation factors, the TURBS is believed to tether the post termination ribosome to the viral RNA for a time necessary for reloading of initiation factors.

Publications reporting on secondary structure prediction, structure probing and (putative) structure/function connections of TURBS elements all provide evidence for a

rather low level of structural organization in the TURBS (15–17,33,34). Stemloops with stems composed of the complementary motif 2*/2 sequences were proposed, which is in agreement with the conservation of the complementarity of these sequences. At least one of the proposed structure models in each of these publications presents a (partially) single stranded motif 1, which has to be accessible when hybridization with the 18S rRNA should occur. In these structures, motif 1 is found on top of a stem composed of the (putative) motif 2*/2 sequences. The lowest number of single stranded motif 1 residues was proposed for the murine norovirus (MNV) TURBS (only 2 ssG) (15). However, the TURBS region predicted to pair with motif 1 in MNV would be located within the ribosome when the latter was positioned at the stop/start site so that motif 1 would be single stranded at this time point. An alternative structure proposed by the same authors would place motif 1 on top of a stem structure composed of the most likely motif 2*/2 sequences. In this structure, a sequence complementary to motif 1 is located close to the latter sequence, but the probing results in part contradict the possible pairing of these residues with motif 1. Taken together, a single stranded motif 1 is at least not unlikely for all these cases.

The results presented in the present study on the RHDV TURBS are consistent with the data on other TURBS elements since we saw a rather low number of paired residues, and in silico analyses predicted different structures of similar free energy that display either paired or single stranded motif 1. However, our probing results clearly argue in favor of a structure with a single stranded motif 1 core sequence GUGGGA. Further support for the importance of single stranded motif 1 was obtained from our 'synthetic' TURBS. The VP2 expression level resulting from TURBS variants with motif 1 complementary sequences closely upstream of motif 1 e.g. in construct p8B was considerably lower than that of construct p8D displaying a single stranded motif 1 in in silico analysis. Our data is also in agreement with the results of foot-printing analyses, in which RHDV mRNA engaged in pre-ternary complex binding showed protection of the GGG in motif 1 whereas cleavage was observed for free RHDV RNA (34).

The functional importance of motif 2*/2 hybridization was first demonstrated via mutation analysis for FCV (17). Experiments conducted with the BM2 TURBS in influenza B virus segment 7 RNA did not lead to unequivocal results as mutation of one side of the putative motif 2*/2 stem reduced reinitiation considerably whereas a change affecting the other side had no influence at all (31). However, the reciprocal exchange with mutations on both sides partially restored BM2 expression, which is at least an indication for the importance of this secondary structure element.

Our experiments [present report and (18)] provided compelling evidence for base pairing of motif 2*/2 and its functional importance in RHDV. Especially the (partial) regain of function by reciprocal exchanges proves the role of duplex formation. An important finding is the identification of crucial stems on both sides of motif 1 in the RHDV TURBS. This is reminiscent of the predicted structure of the FCV TURBS, which has also two stems flanking the single stranded region (17). In comparison with RHDV, the single stranded part of the structure is considerably longer in FCV with the single stranded motif 1 followed by an unpaired stretch of 6 nucleotides and the second stem downstream thereof. Also for FCV the mutagenesis leading to destabilization of either of the two stems resulted in strong reduction of VP2 expression. Interestingly, deletion of the complete structured region downstream of motif 1 resulted in reinitiation at almost wt levels (17). Introduction of an equivalent deletion into the RHDV TURBS led to almost complete abrogation of VP2 expression (not shown) proving that the second stem is crucial for reinitiation in RHDV. Only smaller deletions downstream of this stem were tolerated with only ∼50% reduction of VP2 expression also in RHDV (constructs p5C and p5D, Figure 5).

To verify that we had identified all elements relevant for TURBS activity by the combination of secondary structure prediction, probing and mutation analyses we tested the validity of our structure/function model with a variety of grossly altered TURBS sequences preserving only the identified necessary elements at their respective positions. The importance of the relative positioning of the different motives within the TURBS had been demonstrated previously (17,18,31). The results of this kind of a gain of function approach showed that we had indeed established functional TURBS elements, and this was again dependent on the identified crucial structural elements. In a last step, we optimized our 'synthetic' TURBS according to structure prediction results to obtain a synthetic TURBS with a fold very similar to the fold we propose here for the original TURBS. For this construct VP2 expression levels close to wt were determined, thus, highlighting that we have indeed elucidated the structure/function relationship in the RHDV TURBS in detail.

When considering the structure of a TURBS, it is important to keep in mind that in contrast to an IRES, a TURBS represents a somewhat kinetic element. An IRES is not translated into a protein sequence and the initiating ribosome is not unwinding the complete structure on its way to the start site [see (19,44–46) for review]. In contrast, the TURBS is located within a coding region. The ribosome has to pass the TURBS sequence to reach the start/stop region and therefore has to destroy all secondary structures while translating the sequence. Accordingly, all crucial secondary structure elements will be unfolded and have to refold again quickly when interaction with the passing ribosome has to occur. This consideration already indicates that long distance interactions of RNA sequences should have no significance for TURBS function. The results of earlier analyses strongly support this hypothesis since gross truncation of the sequences upstream of the TURBS did not abrogate efficient reinitiation and the sequence expressed via reinitiation could be replaced by foreign sequences (13,14,17,31,40). Thus, local secondary structures folding rapidly after denaturation of the RNA should be responsible for TURBS function. In this process, the motif 2/2* interaction seems to represent kind of a building block for the TURBS structure. Elimination of the motif 2 sequence (CCUGGGGGG) resulted in detection of increased double strand formation in structure probing experiments for different parts of the TURBS. Interestingly, the motif 1 sequence stayed single stranded in this deletion mutant but, nevertheless, VP2 expression was basically blocked (data not shown).

We demonstrate here, that the motif 2*/2 interaction projecting a (mainly) single stranded motif 1 is the only crucial structure of the RHDV TURBS. It can be hypothesized that this stemloop can refold indeed quickly after the ribosome has passed over it and directs the motif 1 into a position prone for interaction with the rRNA in the small ribosomal subunit. For RHDV, double stranded regions flanking motif 1 on both sides are important whereas the FCV TURBS is even fully functional when only the short lower stem and motif 1 are present (17). It might, however, be that the ∼4 times higher reinitiation efficiency of the RHDV TURBS is due to the much more rigid structure. Overall, it seems logical that the low degree of structure requirements in TURBS reflects the rather specialized and simple task these elements have to fulfill.

The eukaryotic TURBS is in part reminiscent of the prokaryotic Shine-Dalgarno (SD) sequence that is also located at a certain distance upstream of the translational start codon and is responsible for binding and positioning of the small ribosomal subunit via hybridization to a sequence in the (16S) ribosomal RNA (47). Even though there is data proposing a secondary structure with a (partially) single stranded SD flanked by two stems in a chloroplast RNA in *Chlamydomonas reinhardtii* RNA (48), the involvement of secondary structure elements seems not mandatory for the function of the SD sequence, in contrast to the data presented for the TURBS here and in other publications. Thus, the details of the molecular mechanisms underlying TURBS versus SD functions appear to be different, which might be a consequence of the different features of the prokaryotic and eukaryotic translation machineries but could also be due to the different demands, namely the achievement of a coupled translational stop and restart by the TURBS versus the *de novo* recruitment of ribosomes for translation initiation by the SD sequence.

SUPPLEMENTARY DATA

Supplementary Data are available at NAR Online.

ACKNOWLEDGEMENTS

The authors thank Gaby Stooß and Rico Jahnke for excellent technical assistance. We are grateful to Sven Erik Behrens, Martin-Luther-University Halle-Wittenberg, for help with establishing the structure probing techniques.

FUNDING

Deutsche Forschungsgemeinschaft [DFG-Me1367/3]. Funding for open access charge: The Friedrich-Loeffler-Institut will pay for the publication using money provided by the German government.
Conflict of interest statement. None declared.

REFERENCES

1. Clarke,I., Estes,M.K., Green,K., Hansman,G.S., Knowles,N., Koopmans,M., Matson,D.O., Meyers,G., Neill,J., Radford,A. *et al.* (2012) Caliciviridae. In: King,AMQ, Adams,MJ, Carstens,EB and Lefkowitz,EJ (eds). *Virus Taxonomy*. Elsevier, Oxford, pp. 977–986.
2. Ohlinger,V.F., Haas,B., Meyers,G., Weiland,F. and Thiel,H.J. (1990) Identification and characterization of the virus causing rabbit hemorrhagic disease. *J. Virol.*, **64**, 3331–3336.
3. Abrantes,J., van der Loo,W., Le Pendu,J. and Esteves,P.J. (2012) Rabbit haemorrhagic disease (RHD) and rabbit haemorrhagic disease virus (RHDV): a review. *Vet. Res.*, **43**, 12.
4. Mutze,G., Cooke,B. and Alexander,P. (1998) The initial impact of rabbit hemorrhagic disease on European rabbit populations in South Australia. *J. Wildl. Dis.*, **34**, 221–227.
5. Clarke,I.N. and Lambden,P.R. (2001) The molecular biology of human caliciviruses. *Novartis. Found. Symp.*, **238**, 180–191.
6. Herbert,T.P., Brierley,I. and Brown,T.D. (1997) Identification of a protein linked to the genomic and subgenomic mRNAs of feline calicivirus and its role in translation. *J. Gen. Virol.*, **78**, 1033–1040.
7. Mitra,T., Sosnovtsev,S.V. and Green,K.Y. (2004) Mutagenesis of tyrosine 24 in the VPg protein is lethal for feline calicivirus. *J. Virol.*, **78**, 4931–4935.
8. Schaffer,F.L., Ehresmann,D.W., Fretz,M.K. and Soergel,M.I. (1980) A protein, VPg, covalently linked to 36S calicivirus RNA. *J. Gen. Virol.*, **47**, 215–220.
9. Sosnovtsev,S.V. and Green,K.Y. (2000) Identification and genomic mapping of the ORF3 and VPg proteins in feline calicivirus virions. *Virology*, **277**, 193–203.
10. Meyers,G., Wirblich,C. and Thiel,H.J. (1991) Genomic and subgenomic RNAs of rabbit hemorrhagic disease virus are both protein-linked and packaged into particles. *Virology*, **184**, 677–686.
11. McFadden,N., Bailey,D., Carrara,G., Benson,A., Chaudhry,Y., Shortland,A., Heeney,J., Yarovinsky,F., Simmonds,P., Macdonald,A. *et al.* (2011) Norovirus regulation of the innate immune response and apoptosis occurs via the product of the alternative open reading frame 4. *PLoS Pathog.*, **7**, e1002413.
12. Sosnovtsev,S.V., Belliot,G., Chang,K.O., Prikhodko,V.G., Thackray,L.B., Wobus,C.E., Karst,S.M., Virgin,H.W. and Green,K.Y. (2006) Cleavage map and proteolytic processing of the murine norovirus nonstructural polyprotein in infected cells. *J. Virol.*, **80**, 7816–7831.
13. Luttermann,C. and Meyers,G. (2007) A bipartite sequence motif induces translation reinitiation in feline calicivirus RNA. *J. Biol. Chem.*, **282**, 7056–7065.
14. Meyers,G. (2003) Translation of the minor capsid protein of a calicivirus is initiated by a novel termination-dependent reinitiation mechanism. *J. Biol. Chem.*, **278**, 34051–34060.
15. Napthine,S., Lever,R.A., Powell,M.L., Jackson,R.J., Brown,T.D. and Brierley,I. (2009) Expression of the VP2 protein of murine norovirus by a translation termination-reinitiation strategy. *PLoS One*, **4**, e8390.
16. Powell,M.L., Brown,T.D. and Brierley,I. (2008) Translational termination-re-initiation in viral systems. *Biochem. Soc. Trans.*, **36**, 717–722.
17. Luttermann,C. and Meyers,G. (2009) The importance of inter- and intramolecular base pairing for translation reinitiation on a eukaryotic bicistronic mRNA. *Genes Dev.*, **23**, 331–344.
18. Meyers,G. (2007) Characterization of the sequence element directing translation reinitiation in RNA of the calicivirus rabbit hemorrhagic disease virus. *J. Virol.*, **81**, 9623–9632.
19. Firth,A.E. and Brierley,I. (2012) Non-canonical translation in RNA viruses. *J. Gen. Virol.*, **93**, 1385–1409.
20. Hofacker,I.L., Stadler,P.F. and Stocsits,R.R. (2004) Conserved RNA secondary structures in viral genomes: a survey. *Bioinformatics*, **20**, 1495–1499.
21. Simmonds,P., Karakasiliotis,I., Bailey,D., Chaudhry,Y., Evans,D.J. and Goodfellow,I.G. (2008) Bioinformatic and functional analysis of RNA secondary structure elements among different genera of human and animal caliciviruses. *Nucleic Acids Res.*, **36**, 2530–2546.
22. Lim,C.S. and Brown,C.M. (2017) Know your enemy: Successful bioinformatic approaches to predict functional RNA structures in viral RNAs. *Front. Microbiol.*, **8**, 2582.
23. Berry,K.E., Waghray,S., Mortimer,S.A., Bai,Y. and Doudna,J.A. (2011) Crystal structure of the HCV IRES central domain reveals strategy for start-codon positioning. *Structure*, **19**, 1456–1466.
24. Filbin,M.E. and Kieft,J.S. (2009) Toward a structural understanding of IRES RNA function. *Curr. Opin. Struct. Biol.*, **19**, 267–276.
25. Imai,S., Kumar,P., Hellen,C.U.T., D'Souza,V.M. and Wagner,G. (2016) An accurately preorganized IRES RNA structure enables

eIF4G capture for initiation of viral translation. *Nat. Struct. Mol. Biol.*, **23**, 859–864.
26. Muhs,M., Hilal,T., Mielke,T., Skabkin,M.A., Sanbonmatsu,K.Y., Pestova,T. V. and Spahn,C.M.T. (2015) Cryo-EM of ribosomal 80S complexes with termination factors reveals the translocated cricket paralysis virus IRES. *Mol. Cell*, **57**, 422–432.
27. Pfingsten,J.S., Costantino,D.A. and Kieft,J.S. (2006) Structural basis for ribosome recruitment and manipulation by a viral IRES RNA. *Science*, **314**, 1450–1454.
28. Quade,N., Boehringer,D., Leibundgut,M., van den Heuvel,J. and Ban,N. (2015) Cryo-EM structure of Hepatitis C virus IRES bound to the human ribosome at 3.9-Å resolution. *Nat. Commun.*, **6**, 7646.
29. Giedroc,D.P., Theimer,C.A. and Nixon,P.L. (2000) Structure, stability and function of RNA pseudoknots involved in stimulating ribosomal frameshifting. *J. Mol. Biol.*, **298**, 167–185.
30. Staple,D.W. and Butcher,S.E. (2005) Pseudoknots: RNA structures with diverse functions. *PLoS Biol.*, **3**, e213.
31. Powell,M.L., Leigh,K.E., Poyry,T.A., Jackson,R.J., Brown,T.D. and Brierley,I. (2011) Further characterisation of the translational termination-reinitiation signal of the influenza B virus segment 7 RNA. *PLoS One*, **6**, e16822.
32. Powell,M.L., Napthine,S., Jackson,R.J., Brierley,I. and Brown,T.D. (2008) Characterization of the termination-reinitiation strategy employed in the expression of influenza B virus BM2 protein. *RNA*, **14**, 2394–2406.
33. Poyry,T.A., Kaminski,A., Connell,E.J., Fraser,C.S. and Jackson,R.J. (2007) The mechanism of an exceptional case of reinitiation after translation of a long ORF reveals why such events do not generally occur in mammalian mRNA translation. *Genes Dev.*, **21**, 3149–3162.
34. Zinoviev,A., Hellen,C.U.T. and Pestova,T.V. (2015) Multiple mechanisms of reinitiation on bicistronic calicivirus mRNAs. *Mol. Cell*, **57**, 1059–1073.
35. Sutter,G., Ohlmann,M. and Erfle,V. (1995) Non-replicating vaccinia vector efficiently expresses bacteriophage T7 RNA polymerase. *FEBS Lett.*, **371**, 9–12.
36. Wyatt,L.S., Moss,B. and Rozenblatt,S. (1995) Replication-deficient vaccinia virus encoding bacteriophage T7 RNA polymerase for transient gene expression in mammalian cells. *Virology*, **210**, 202–205.
37. Sambrook,J. and Russell,D.W. (2001) *Molecular Cloning: A Laboratory Manual*. Cold Spring Harbor Laboratory, N.Y.
38. Wirblich,C., Thiel,H.J. and Meyers,G. (1996) Genetic map of the calicivirus rabbit hemorrhagic disease virus as deduced from in vitro translation studies. *J. Virol.*, **70**, 7974–7983.
39. Schägger,H. and Jagow,G.v. (1987) Tricine- sodium dodecyl sulfate-polyacrylamide gel electrophoresis for the separation of proteins in the range from 1 to 100 kDa. *Anal. Biochem.*, **166**, 368–379.
40. Luttermann,C. and Meyers,G. (2014) Two alternative ways of start site selection in human norovirus reinitiation of translation. *J. Biol. Chem.*, **289**, 11739–11754.
41. Thirumalai,D. (1998) Native secondary structure formation in RNA may be a slave to tertiary folding. *Proc. Nat. Acad. Sci. U.S.A.*, **95**, 11506–11508.
42. Wessner,D.R. (2010) Discovery of the Giant Mimivirus. *Nat. Education*, **3**, 61.
43. Schneider,R.J. and Mohr,I. (2003) Translation initiation and viral tricks. *Trends Biochem. Sci.*, **28**, 130–136.
44. Lozano,G. and Martinez-Salas,E. (2015) Structural insights into viral IRES-dependent translation mechanisms. *Curr. Opin. Virol.*, **12**, 113–120.
45. Martinez-Salas,E., Francisco-Velilla,R., Fernandez-Chamorro,J. and Embarek,A.M. (2017) Insights into Structural and Mechanistic Features of Viral IRES Elements. *Front. Microbiol.*, **8**, 2629.
46. Martinez-Salas,E., Ramos,R., Lafuente,E. and Lopez de Quinto,S. (2001) Functional interactions in internal translation initiation directed by viral and cellular IRES elements. *J. Gen. Virol.*, **82**, 973–984.
47. Shine,J. and Dalgarno,L. (1975) Determinant of cistron specificity in bacterial ribosomes. *Nature*, **254**, 34–38.
48. Mayfield,S.P., Cohen,A., Danon,A. and Yohn,C.B. (1994) Translation of the psbA mRNA of Chlamydomonas reinhardtii requires a structured RNA element contained within the 5′ untranslated region. *J. Cell Biol.*, **127**, 1537–1545.